Int J Adv Manuf Technol (2015) 76:1163–1172
DOI 10.1007/s00170-014-6338-x

ORIGINAL ARTICLE

Experimental investigation and statistical optimization of laser surface cladding parameters

Javad Marzban · Pouya Ghaseminejad · Mohamad Hasan Ahmadzadeh · Reza Teimouri

Received: 1 April 2014 / Accepted: 2 September 2014 / Published online: 14 September 2014

Abstract In laser surface cladding process, the formed clad geometry is directly affected by laser cladding parameters like laser power, scan speed, and powder feed rate. Therefore, finding an optimal parameter setting to increase the process performance is crucial. In the present study, experimental investigation on laser cladding process of AISI 1040 has been performed. Here, numbers of nine experiments were designed and conducted based on L_9 orthogonal array design to study effects of mentioned factors on clad height, clad width, and clad depth. Then the principal component analysis (PCA) was integrated with TOPSIS method for multiresponses optimization of laser cladding process. Here, the PCA was used to find appropriate weight factor related to each quality characteristic. Hereafter, the technique for order preference by similarity to ideal solution (TOPSIS) was utilized to find optimal solutions. Confirmatory experiments were carried out to validate optimal results. Results revealed that the laser power has greatest influence on laser cladding quality characteristics. Furthermore, results which were obtained through of confirmatory experiments reveal that the developed method can effectively acquire the optimal combination of laser cladding parameters.

Keywords Laser cladding · Multiresponses optimization · Cladding parameters

J. Marzban
Department of Automation Engineering, Iran University of Science and Technology, Tehran, Iran

P. Ghaseminejad · M. H. Ahmadzadeh
Department of Mechanical Engineering, Islamic Azad University, Dezfull branch, Dezfull, Iran

R. Teimouri (✉)
Department of Mechanical Engineering, Babol University of Technology, Babol, Iran
e-mail: reza_teimoori@yahoo.com

1 Introduction

Laser cladding [1, 2] is a process that can manufacture a metallurgical bonded coating on the substrate by injecting one certain clad material into the other, for the sake of more advanced material properties or the repair of critical components with a laser beam as the heating source. The main process parameters of laser cladding are laser power, spot size, laser scanning speed, and powder feed rate. Potentially different combinations of these parameters can produce different effects on the cladding geometries and characteristics, i.e., layer width, height, and microstructure with high quality. Moreover, improper parameter combination would also bring out great residual stress that probably has a detrimental impact on the performances of the workpiece.

In laser cladding process, clad geometry is defined by clad depth (D), clad width (W), and clad height (H). The defined geometry is highly affected by variation of process parameters. Figure 1 presents the clad geometry characteristics. To get clad layer with high quality, it is highly desirable that laser cladding can provide a strong intermixture and metallurgical bond with minimum dilution (e.g., $D/(D + H)$). The main challenge of achieving lower dilution is how to choose the process parameters that can produce a good clad layer with the required cladding geometry.

Recently, numbers of studies have been performed to investigate the effect of process parameters of laser cladding. The majority of these studies have focused on the effect of one or several parameters on the coating microstructure, temperature field, residual stress, or other mechanical properties [3–7], for example, the effect of laser power on the cladding temperature field and the heat affected zone, adaptive tool path deposition, and the relation between the cladding angle and the shape of cladding track. A few studies are performed on finite element modeling (FEM) and experimental verification for clad geometry control [8–12]. The advantage of dilution control based on FEM is that

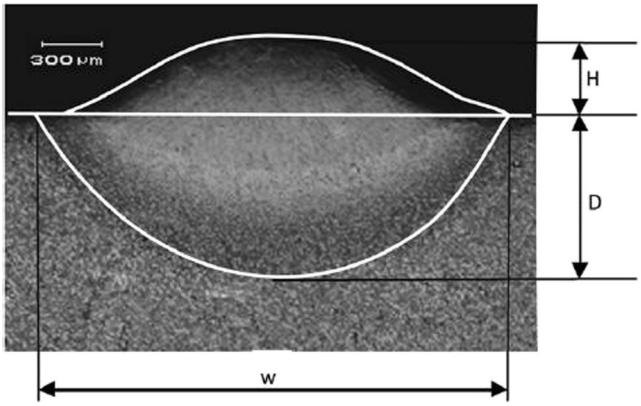

Fig. 1 Dimensional characteristics of clad profile geometry [20]

one can understand the thermophysical properties of cladding coatings and substrate materials deeply. However, it requires a detailed knowledge and exact model of laser cladding process for specified cladding coatings and substrate material. The majority of these studies reported only one or two process conditions such as laser power and/or powder feed rate; therefore, it is hard to find a good parametric combination under the premise of keeping other parameters constant. However, the statistical analysis method is a successful alternative to investigate the relations between cladding geometry and its input parameters. Although, the statistical analysis were successfully applied on laser manufacturing process such as laser welding [13–15], laser hardening [16], and laser cutting [17–19], there is still lack of the application of statistical analysis method on laser cladding process. There are just few researches which associated statistical analysis with laser surface cladding process. Sun and Hao [20] applied response surface methodology along with desirability approach function to improve cladding quality characteristics in Ti6Al4V laser cladding. Mondal et al. [21] applied gray relational analysis to statistically optimize laser cladding factors.

In this paper, a series of statistical methods are applied to investigate optimal combination of laser power, scan speed, and powder feed rate to minimize clad depth and clad height as well as maximize the clad width. For this purpose, firstly principal component analysis (PCA) is applied on experimental data to find appropriate weight factors of each response. Then, the technique for order preference by similarity to ideal solution (TOPSIS) is used to find optimal combination of process factors. Finally, confirmatory experiments are carried out to verify the optimal process parametric combination as predicted by PCA-TOPSIS.

2 Methodologies

2.1 Principal component analysis

The principal component analysis is a collection of statistic analysis that is used to find importance of quality characteristics in a certain system such as manufacturing processes [22]. The procedure is described as follows:

(a) The original multiple quality characteristic array

$$x_i(j),\ i=1,2,\ldots,m;\ j=1,2,\ldots,n$$
$$X=\begin{bmatrix} x_1(1) & x_1(2) & \ldots & \ldots & x_1(n) \\ x_2(1) & x_2(2) & \ldots & \ldots & x_2(n) \\ \ldots & \ldots & \ldots & \ldots & \ldots \\ x_m(1) & x_m(2) & \ldots & \ldots & x_m(n) \end{bmatrix} \quad (1)$$

Where m is the number of experiment and n is the number of the quality characteristic. In this paper, x is the gray relational coefficient of each quality characteristic. In this paper, m=18 and n=2.

(b) Correlation coefficient array

The correlation coefficient array is evaluated as follows:

$$R_{jl}=\left(\frac{Cov(x_i(j),x_i(l))}{\sigma_{x_i}(j)\times\sigma_{x_i}(l)}\right),\ j=1,2,\ldots,n;\ l=1,2,\ldots,n \quad (2)$$

Where $Cov(x_i(j), x_i(l))$ is the covariance of sequences $x_i(j)$ and $x_i(l)$. $\sigma_{xi}(j)$ is the standard deviation of sequence $x_i(j)$ and $\sigma_{xi}(l)$ is the standard deviation of sequence $x_i(l)$.

(c) Determining the eigenvalues and eigenvectors

The eigenvalues and eigenvectors are determined from the correlation coefficient array according to following equation:

$$(R-\lambda_k I_m)V_{ik}=0 \quad (3)$$

Where λ_k is eigenvlues, $\sum_{k=1}^{n}\lambda_k=n$, k=1,2,…,n; $V_{ik}=[a_{k1},a_{k2},\ldots a_{kn}]^T$ is eigenvectors corresponding to the eigenvalue λ_k.

(d) Principal component

The uncorrelated principal component is formulated as follows:

$$Y_{mk}=\sum x_m(i).V_{ik} \quad (4)$$

The principal components are aligned in descending order with respect to variance, and therefore the first principal component Y_{m1} accounts for most variance in the data.

2.2 Technique for order preference by similarity to ideal solution

The technique for order preference by similarity to ideal solution (TOPSIS) is a simple method which considered that the chosen alternative should have the shortest distance from the ideal solution and the longest distance from the negative ideal solution [23].

The main procedure of TOPSIS method for selection of the best alternative from among those available is described as follows:

Step 1 Calculate the normalized decision matrix, $R=[r_{ji}]_{m\times n}$

$$r_{ij}=\frac{x_{ij}}{\sqrt{\sum_{j=1}^{m}x_{ij}^2}},\quad i=1,2,\ldots,m;\ \text{and}\ j=1,2,\ldots,n \tag{5}$$

Where i is number of experiment (e.g., in the present study m=9) and j is number of responses (e.g., in the present study n=3).

Step 2 Calculation of weighted normalized decision matrix, $V=[v_{ij}]_{m\times n}$

$$v_{ij}=w_{ij}\times r_{ij} \tag{6}$$

Where the w_{ij} are the weight factors which are calculated from principal component analysis.

Step 3 Determination of the ideal and negative ideal solution

(a) For ideal solution

$$V^{+}=\left\{\left[\max\left(v_{ij}\right),j\in J\right]\ \text{or}\ \left[\min\left(v_{ij}\right),j\in J'\right]\right\}=\left[V_1^{+},V_2^{+},V_3^{+}\right] \tag{7}$$

(b) For negative-ideal solution

$$V^{-}=\left\{\left[\min\left(v_{ij}\right),j\in J\right]\ \text{or}\ \left[\max\left(v_{ij}\right),j\in J'\right]\right\}=\left\{V_1^{-},V_2^{-},V_3^{-}\right\} \tag{8}$$

Where $J=\{j=1, 2, 3\}$ associated with higher the better performance such as clad width, and $J'=\{j=1, 2, 3\}$ associated with lower the better performance like clad height and clad depth.

Step 4 Calculation of separation measure

The separation of each alternative from the ideal solution is given as

$$S_i^{+}=\sqrt{\sum_{j=1}^{n}\left(v_{ij}-V_j^{+}\right)^2}\,i=1,2,\ldots 9 \tag{9}$$

The separation of each alternative from the negative-ideal solution is given as

$$S_i^{-}=\sqrt{\sum_{j=1}^{n}\left(v_{ij}-V_j^{-}\right)^2}\,i=1,2,\ldots 9 \tag{10}$$

Step 5 Calculation of relative closeness of a particular alternative to ideal solution can be expressed as:

$$C_i^{+}=\frac{S_i^{-}}{S_i^{-}+S_i^{+}} \tag{11}$$

Step 6 Ranking of the preference order is to be carried out. The value of C_i^{+} indicates the most preferred and least preferred feasible solution. In other word, the combination of factors that causes higher C_i^{+} is the most optimal solution.

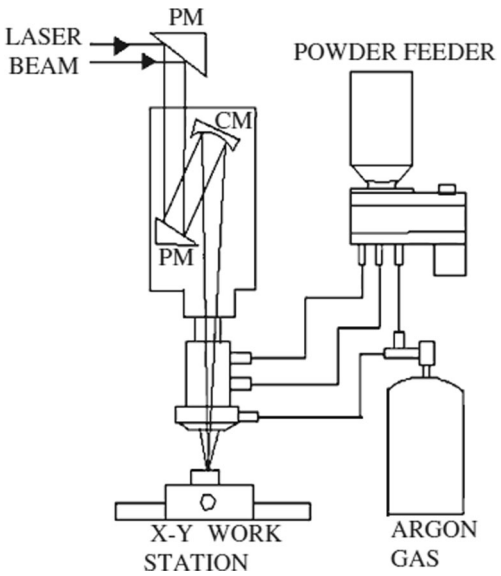

Fig. 2 A schematic view of laser cladding machine [21]

Table 1 Process variables and responses

Process factors	Unit	Symbol	Level 1	Level 2	Level 3
Laser power	kW	*P*	1	1.25	1.5
Scan speed	m/min	*S*	0.2	0.5	0.8
Powder feed rate	mg/min	*f*	5	8	11

3 Experimentations

3.1 Experimental equipments

The experiments were performed on a 3.5 kW pulsed wave CO_2 laser machine. The machine includes a high-power laser system along with laser beam delivery system, powder feeding unit, and CNC machine table manipulator. Figure 2 reveals a schematic view of laser cladding process. A combination of Ni-Cr-Mo powders is fed into a molten pool using volumetric controlled powder feeder through a coaxial powder feeding nozzle. The powders are firstly dried at 120 °C for 5 h. Here, argon is used as a shielding gas and powder carrier.

3.2 Experimental material and procedure

Experiments are carried out on AISI 1040 as substrate workpiece material. The substrates are plates with dimensions of $110\times110\times13$ mm^3 which are grinded with sandpapers to get rid of the impurity on the surface. Combination of nickel, chromium, and molybdenum powder is used as cladding material with the granularity of 90 μm (180 mesh).

In the present study, a single-pass experiment of laser cladding was totally performed with nine sets of process parameters. Hence, nine cladding tracks were deposited in random order every time. After the experiments, the plates with cladding coatings should be cut off into several pieces perpendicular to cladding tracks and each cross-section of these pieces were polished to a mirror finish through diamond paste with a granularity of 1–2 μm. Then these pieces could be finally used to measure the cladding geometry with an optical microscope. The measured profile parameters, namely experimental responses, were the average values of the corresponding results of the experiments.

3.3 Experimental plan

According to the literatures and our laboratory experiences, the most predominant factors which have great influence on the clad geometry were identified. They were laser power, scanning speed, and powder feed rate. Prior to the design of experiments, the ranges of process parameters in laser cladding should be determined based on the equipment conditions and preliminary studies. Except the fixed parameters, each process parameter used for optimization is limited in a design domain. Here, due to the equipment limitation, the laser spot size is fixed and thus laser power, scanning speed, and powder feed rate are selected as adjustable parameters. About the spot size, it should be explained that it refers to diameter of the laser nuzzle. In a pulsed laser cladding process, when the spot size goes beyond a critical value, the overlapping occurs in clad surface and causes excessive heat input which evaporates particles in flame which increases the clad depth. On the other hand at low spot size, gap between spots occur in clad surface that does not coat the substrate surface as well. However, in the present study, the laser machine has limitation in the spot size. It means that the spot size cannot be adjusted and regulated due to machine limitation. Therefore, it was fixed at 2 mm.

To investigate the effect of these parameters, a L_9 (3^3) Taguchi orthogonal design is developed using the statistical software MINITAB 14. Each factor is varied over three levels. Here, numbers of nine experiments were conducted to analyze the experimental data acquired from the measured responses and corresponding process parameters. The main reason for using L_9 is to prevent high cost of experiments. Generally, the laser materials processing operations are very expensive. About the laser cladding process, it should be explained that preparation of powders and measurement of responses (i.e., clad height, clad width, and clad depth) need precise polishing operations and metallographic examinations. Therefore, selection of full factorial

Table 2 Design matrix layout and measure responses

No	*P* (kW)	*S* (m/min)	*f* (mg/min)	Clad height (mm)	Clad width (mm)	Clad depth (mm)
1	1	0.2	5	0.18333	3.11	0.41
2	1	0.5	8	0.13333	2.71667	0.2
3	1	0.8	11	0.17667	3.39333	0.3
4	1.25	0.2	8	0.23333	2.57333	0.25
5	1.25	0.5	11	0.29667	4.25333	0.55
6	1.25	0.8	5	0.19	3.68667	0.25
7	1.5	0.2	11	0.2333	4.19	0.25
8	1.5	0.5	5	0.251	4.63667	0.375
9	1.5	0.8	8	0.36333	4.74	0.53

Fig. 3 Effect of laser cladding parameters on clad height

design (i.e., 3^3=27 experiments) increases the experimental costs drastically. Hence, in this paper, the L_9 orthogonal design was used to decrease the prices of experiments for at least three times.

Table 1 presents laser cladding predominant variables along with their working levels. Also, Table 2 is a design matrix with measured values of responses.

4 Results and discussion

4.1 Effects of cladding parameters on clad quality characteristics

4.1.1 Analysis of clad height

Figure 3 presents effects of process factors on clad height. It is seen that increase in laser power has negative effect on clad height. It means that the clad height increases at higher laser power. At higher laser power, more thermal energy is transferred to powders on substrate. Hence, it increases numbers of molten particles on a substrate and their accumulation cause higher clad height.

From Fig. 3, it is inferred that increase in scan speed causes lower clad height. At higher scan speeds, less metal powders are injected on a substrate. Also, lower thermal energy transfers to powder. Hence, numbers of non-molten particles on substrate increase and that cause low clad height.

Figure 3 reveals that by increasing powder feed rate, the clad height increases and reaches to a maximum value at 8 mg/min; then by further increase in powder feed rate, the effect is saturated. This effect can be attributed to this reason. Increasing powder feed rate results in more metal powder flooding to substrate. The powder coating deposited on substrate becomes higher while absorbing more laser energy. As a

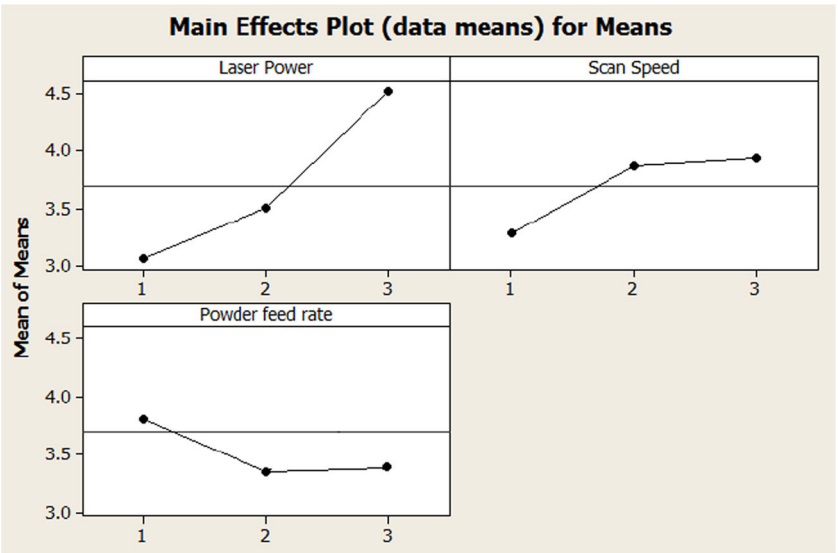

Fig. 4 Effect of laser cladding parameters on clad width

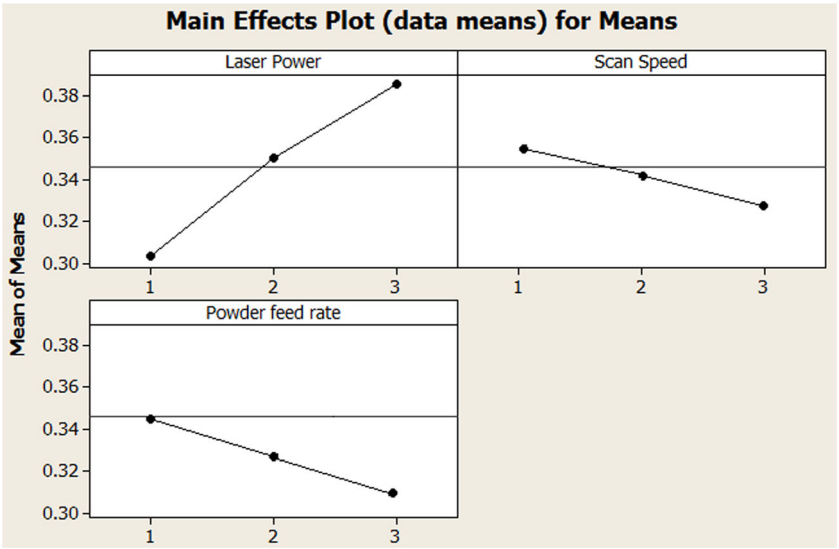

Fig. 5 Effect of laser cladding parameters on clad depth

result, more power is used to melt the metal powder instead of substrate, which consequently brings high cladding bead. When powder feed rate goes beyond 8 mg/min, due to a large number of powders on substrate, the number of nonmolten particles also increases and the melting efficiency decreases to some extent. Therefore, no more increase in clad height is observed.

4.1.2 Analysis of clad width

Figure 4 depicts effects of laser cladding parameters on clad width. It is seen from this figure that laser power has positive effect on clad width. This effect can be attributed for this reason. At higher laser power, transferring more thermal power to powders causes increase in the number of molten particles and thicker clad. Hence, deposition of metal powder on a substrate improves and thicker clad is formed. Hence, clad width increases.

According to Fig. 4, it is seen that high scan speed results in high clad width. In other word, increase in scan speed has slightly positive effect on clad width. As discussed, at higher scan speed, less metal powders are injected on a substrate and thinner layer of coating is formed. If more power is absorbed by substrate, it will give birth to a wider melt pool and then a greater clad width is formed.

Figure 4 shows effect of powder feed rate on clad width. It is seen from this figure that by increasing the powder feed rate, the clad width firstly decreases and reaches to a minimum value at 8 mg/min. Then by further increases in powder feed rate, the effect of powder feed rate on clad width is saturated. As explained, by increasing the powder feed rate, overflow of powders leads to absorbent of more laser energy. Therefore, more power is used to melt the metal powder instead of substrate. Thus, clad width decreases. Also, by further increasing the powder feed rate, no more reduction is observed in bead width value.

4.1.3 Analysis of clad depth

Figure 5 presents effect of laser cladding parameters on clad depth. According to this figure, it is seen that the clad depth increases by increasing the laser power. By increasing the laser power, due to increase in thermal energy, more metal powder and substrate material are melted. Hence, the molten substrate diffuses into beneath layers. Hence, the clad depth increases.

According to Fig. 5, it is inferred that both the scan speed and powder feed rate result in the reduction of clad depth. Those effects are attributed to the following reasons. Higher scanning speed can reduce the heat input rate and then less laser energy is absorbed by substrate at the same period,

Table 3 Eigenvalues and explained variations for principal component

Principal component	Eigenvalues	Explained variations (%)
First	2.4315	81.05
Second	0.1886	6.29
Third	0.3798	12.66

Table 4 Eigenvectors for principal component

Quality characteristic	Eigenvectors		Third principal component
	First principal component	Second principal component	
Clad height	0.6010	0.7951	0.0809
Clad width	0.5599	−0.3466	−0.7526
Clad depth	0.5704	−0.4976	0.6335

Table 5 The contribution of each individual quality characteristic for the first principal component

Quality characteristic	Contribution
Clad height	0.3612
Clad width	0.3135
Clad depth	0.3254

resulting in decreased molten depth. By increasing the powder feed rate, more powder material covers the substrate and less laser energy is injected into the substrate. It means that the high laser energy melts metal powders instead of substrate, hence the molten depth of laser cladding process decreases.

From the above figures and their discussions, it is understood that laser cladding factors have uncontrollable manner on clad quality characteristics. Hence, finding optimal parameters combination to maximize clad width and minimize clad depth simultaneously is really complex and using an appropriate multiresponses optimization method is needed. Therefore, in the present study, the TOPSIS-PCA method is used to find appropriate weight factors for each quality characteristic and best optimal solutions to improve the laser cladding performance.

4.2 Optimization of process parameters to reach desirable clad quality characteristics

4.2.1 Finding appropriate weight factors of each response using PCA

In the present paper, in order to objectively reflect the relative importance for each performance characteristic in TOPSIS, principal component analysis is specially introduced here to determine the corresponding weighting values for each performance characteristic. The elements of the array for multiple performance characteristics listed in Table 2 represents the obtained value of each performance characteristic. These data are used to evaluate the correlation coefficient matrix, and determine the corresponding eigenvalues, that is shown in Table 3. The eigenvector (Table 4) corresponding to each eigenvalue is listed in Table 5, and its square can represent the contribution of the corresponding performance characteristic to the principal component. Table 6 shows that the contributions of clad height, clad width, and clad depth are 0.3612, 0.3135, and 0.3254, respectively. Moreover, the variance contribution for the first principal component characterizing the whole original variables, i.e., the three performance characteristics, is as high as 81.05 %. Hence, for this study, the squares of its corresponding eigenvectors are selected as the weighting values of the related performance characteristic, and the coefficients w_1, w_2, and w_3 for constructing TOPSIS tables are thereby set as 0.3612, 0.3135, and 0.3254, respectively.

4.2.2 Optimization of clad quality characteristics by TOPSIS

In optimization by TOPSIS, firstly, the design matrix should be normalized and then weighed using Eqs. 5 and 6. In other word, the normalized matrix is calculated by Eq. 5 and then weighed by multiplying normalized matrix and weight factors which were obtained through PCA (i.e., w_1=0.3612, w_2=0.3135, and w_3= 0.3254). Table 6 presents normalized matrix and weighed matrix of performance characteristics.

The next step is to determine ideal and negative ideal solutions from the weighed normalized quality characteristics in Table 7 according to Eqs. 7 and 8. Therefore, the ideal solutions and negative ideal solutions arrays are V^+={0.0674, 0.1311, and 0.0592} and V^-={0.1837, 0.0712, and 0.1627}, respectively.

After determining ideal and negative ideal solutions, the separation measures must be calculated using Eqs. 9 and 10. Then relative closeness of a particular

Table 6 Normalized and weighed data of performance characteristics

No	Normalized quality characteristics			Weighed normalized quality characteristics		
	Clad height	Clad width	Clad depth	Clad height	Clad width	Clad depth
1	0.2566	0.2475	0.3728	0.0927	0.0860	0.1213
2	0.1866	0.2398	0.1818	0.0674	0.0752	0.0592
3	0.2472	0.2995	0.2728	0.0893	0.0939	0.0888
4	0.3265	0.2271	0.2273	0.1179	0.0712	0.0740
5	0.4152	0.3754	0.5001	0.1500	0.1177	0.1627
6	0.2659	0.3254	0.2273	0.0960	0.1020	0.0740
7	0.3265	0.3698	0.2273	0.1179	0.1159	0.0740
8	0.3513	0.4092	0.3410	0.1269	0.1283	0.1109
9	0.5085	0.4183	0.4819	0.1837	0.1311	0.1568

Table 7 Calculated ideal and negative ideal separation measures along with relative closeness

No	S_i^+	S_i^-	C_i^+
1	0.0808	0.1011	0.5557
2	0.0559	0.1557	0.7359
3	0.0523	0.1220	0.6998
4	0.0797	0.1104	0.5807
5	0.1331	0.0574	0.3014
6	0.0434	0.1285	0.7475
7	0.0548	0.1191	0.6851
8	0.0789	0.0985	0.5483
9	0.1518	0.0602	0.2839

alternative to ideal solution can be calculated using Eq. 11. Table 6 presents the separation measures (i.e., S_i^+ and S_i^-) along with relative closeness of a particular alternative to ideal solution.

As it is seen in Table 7, by using the proposed method, the optimization design can be desirably performed with respect to a single relative closeness of a particular alternative to ideal solution rather than complicated performance characteristics. It means that this method converts a multiple performance optimization problem to a single performance one.

The response table of Taguchi method is employed here to calculate the average relative closeness for each laser cladding parameter level. It is done by sorting the relative closeness corresponding to levels of the laser cladding parameter in each column of the orthogonal array, and taking an average on those with the same level. Figure 6 presents the response of process factors for relative closeness.

Basically, the larger the value of relative closeness implies, the better the corresponding multiple performance characteristic. Accordingly, the level that gives the largest average response is selected. From Fig. 6, the best combination of the coating parameters is P_1 (first level of laser power), S_2 (second level of scan speed), and f_2 (second level of powder feed rate). Also, this figure depicts that the laser power has the greatest effect on cladding quality characteristics. Also, the contribution of powder feed rate and scan speed on quality characteristics are equal to some extent.

4.2.3 Confirmatory experiments

Once the optimal level of the cutting parameters is identified, the following step is to verify the improvement of the performance characteristics using this optimal combination. The estimated relative closeness using the optimal level of the design parameters can be calculated using the following equation.

$$\gamma^* = \gamma_m + \sum_{i=1}^{o} \left(\gamma_i' - \gamma_m\right) \tag{12}$$

Where γ^* is the estimated gray relational grade, γ_m is the total mean gray relational grade, γ_i' is the mean gray relational grade at the optimal level, and o is the number of the main design parameters that affect the quality characteristics.

Table 8 compares the results of the confirmation experiments using the optimal cladding parameters (P_1 S_2 f_2) obtained by the proposed method and with those of the initial laser cladding parameters (P_1 S_1 f_1). It is seen from Table 8 that using optimal combination of factors results in 24.65 % improvement in relative closeness from the initial parameter setting. This proves

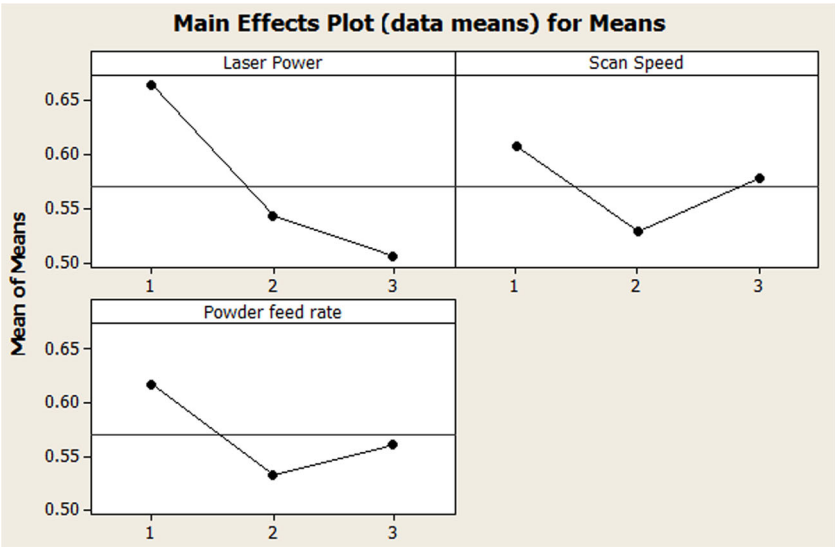

Fig. 6 Response of process factors to relative closeness of a particular alternative to ideal solution

Table 8 Results of confirmatory experiment

	Initial laser cladding parameters	Optimal laser cladding parameters	
		Experiment	Prediction
Setting level	$P_1\ S_1\ f_1$	$P_1\ S_2\ f_2$	$P_1\ S_2\ f_2$
Clad height	0.18333	0.13333	–
Clad width	3.11	2.71667	–
Clad depth	0.41	0.2	–
Means of relative closeness	0.5557	0.7375	0.7375

Improvement relative closeness from first setting level to optimal setting level=24.65 %

the utility of the proposed approach in relation to product/process optimization, where more than one objective has to be fulfilled simultaneously.

5 Conclusion

In this paper, the application of collections of statistical techniques to optimize the laser cladding process with the multiple performance characteristics has been reported. An expression of statistical techniques directly integrates the multiple performance characteristics (i.e., clad height, clad width, and clad depth) into a single performance characteristic that is called relative closeness. Therefore, optimization of the complicated multiple performance characteristics can be greatly simplified to a single objective optimization problem through this approach. It is found that the mentioned performance characteristics are improved together using this methodology.

Furthermore, other obtained results can be summarized as follows:

1. Increasing laser power has positive effect on clad width on the one hand, and it has negative effect on laser height and laser depth on the other hand.
2. Increasing scan speed has positive effect on laser clad height, clad width, and clad depth.
3. Increasing powder feed rate has negative effect on clad height and clad width on the one hand, and it has positive effect on clad depth on the other hand.
4. The combination of 1-kW laser power, 0.5 m/min scan speed, and 8 mg/min powder feed rate results in most desirable clad quality characteristics. This result has been verified with confirmatory experiment that implies efficiency and effectiveness of proposed methodology.

References

1. Deus D (2004) A thermal and mechanical model of laser cladding. Dissertation Abstracts International 65–04 (Section: B); Chapter 1
2. Price JWH, Ziara-Paradowska A, Joshi S, Finlayson T, Semetay C, Nied H (2008) Comparison of experimental and theoretical residual stresses in welds: the issue of gauge volume. Int J Mech Sci 50(3): 513–521
3. Luo F, Yao JH, Hu XX, Chai GZ (2011) Effect of laser power on the cladding temperature field and the heat affected zone. J Iron Steel Res Int 18(1):73–78
4. Qi H, Azer M, Singh P (2010) Adaptive tool path deposition method for laser net shape manufacturing and repair of turbine compressor airfoils. Int J Adv Manuf Technol 48(1):121–131
5. Onwubolu GC, Davim JP, Oliveira C, Cardoso A (2007) Prediction of clad angle in laser cladding by powder using response surface methodology and scatter search. Opt Laser Technol 39(6):1130–1134
6. Kumar A, Roy S (2009) Effect of three-dimensional melt pool convection on process characteristics during laser cladding. Comput Mater Sci 46(2):495–506
7. Dubourg L, St-Georges L (2006) Optimization of laser cladding process using Taguchi and EM methods for MMC coating production. J Therm Spray Technol 15(4):790–795
8. Hofman JT, de Lange DF, Pathiraj B, Meijer J (2011) FEM modeling and experimental verification for dilution control in laser cladding. J Mater Process Technol 211(2):187–196
9. Long RS, Liu WJ, Xing F, Wang HB (2008) Numerical simulation of thermal behavior during laser metal deposition shaping. Trans Nonferrous Metals Soc China 18(3): 691–699
10. Palumbo G, Pinto S, Tricarico L (2004) Numerical finite element investigation on laser cladding treatment of ring geometries. J Mater Process Technol 155–156:1443–1450
11. Zhao HY, Zhang HT, Xu CH, Yang XQ (2009) Temperature and stress fields of multi-track laser cladding. Trans Nonferrous Metals Soc. China 19(Suppl. 2):s495–501
12. Zhu WD, Liu QB, Li HT, Zheng M (2007) A simulation model for the temperature field in bioceramic coating cladded by wide-band laser. Mater Des 28(10):2673–2677
13. Benyounis KY, Olabi AG (2008) Optimization of different welding processes using statistical and numerical approaches—a reference guide. Adv Eng Softw 39(6):483–496
14. Benyounis KY, Olabi AG, Hashmi MSJ (2005) Effect of laser welding parameters on the heat input and weld-bead profile. J Mater Process Technol 164–165:978–985
15. Benyounis KY, Olabi AG, Hashmi MSJ (2005) Optimizing the laser-welded butt joints of medium carbon steel using RSM. J Mater Process Technol 164–165:986–989
16. Hamad AR, Abboud JH, Shuaeib FM, Benyounis KY (2010) Surface hardening of commercially pure titanium by laser nitriding: response surface analysis. Adv Eng Softw 41(4): 674–679
17. Choudhury IA, Shirley S (2010) Laser cutting of polymeric materials: an experimental investigation. Opt Laser Technol 42:503–508
18. Dhupal D, Doloi B, Bhattacharyya B (2009) Modeling and optimization on Nd:YAG laser turned micro-grooving of cylindrical ceramic material. Opt Lasers Eng 47:917–925
19. Kuar AS, Doloi B, Bhattacharyya B (2006) Modeling and analysis of pulsed Nd:YAG laser machining characteristics during micro-drilling of zirconia (ZrO_2). Int J Mach Tools Manuf 46:1301–1310

20. Sun Y, Hao M (2012) Statistical analysis and optimization of process parameters in Ti6Al4V laser cladding using Nd:YAG laser. Opt Lasers Eng 50:985–995
21. Mondal S, Paul CP, Kukreja LM, Bandyopadhyay PPK (2013) Application of Taguchi-based gray relational analysis for evaluating the optimal laser cladding parameters for AISI1040 steel plane surface. Int J Adv Manuf Technol 66:91–96
22. Lu HS, Chang CK, Hwang NC, Chung CT (2009) Grey relational analysis coupled with principal component analysis for optimization design of the cutting parameters in high-speed end milling. J Mater Process Technol 209:3808–3817
23. Sivapirrakasam SP, Mathew J, Surianarayanan M (2011) Multi-attribute decision making for green electrical discharge machining. Expert Syst Appl 38:8370–8374